

NEUTRON SPECTROSCOPY AT THE SURFACE OF SATURN'S MOON TITAN

Patrick N. Peplowski^{1*}, Jack T. Wilson¹, Mauricio Ayllon-Unzueta², Anna Engle^{1,3}, Ralph D. Lorenz¹, Shannon M. MacKenzie¹, Scott L. Murchie¹, David J. Lawrence¹, Ann M. Parsons², Elizabeth P. Turtle¹, and Zachary W. Yokley¹.

¹ Johns Hopkins Applied Physics Laboratory, Laurel MD 20723 USA (*Patrick.Peplowski@jhuapl.edu), ² NASA Goddard Space Flight Center, Greenbelt, MD 20771 USA, ³ Northern Arizona University, Flagstaff, AZ 86011 USA.

Introduction: Planetary neutron spectroscopy developed within the context of quantifying concentrations of water on terrestrial planets and rocky asteroids. In this geochemical scenario, water (H₂O) and hydroxyl (OH) are the dominant hydrogen-bearing species in otherwise silicate, hydrogen-poor surfaces. This paradigm fails when applied to Titan, whose surface which is expected to be composed of admixtures of water and ammonia (NH₃) ices, liquid methane (CH₄), and complex organic compounds – all of which contain hydrogen. Neutron spectroscopy with DraGNS therefore requires a different framework than that used to interpret data from Mars, the Moon, and Mercury.

Starting from fundamental neutron moderation and absorption theory, we provide a framework for interpreting neutron spectroscopic measurements made on the surface of Titan. We are currently validating this framework via a set of laboratory measurements of Titan-surface analog materials, as well as simulations that closely replicate the planned implementation of the Dragonfly Gamma-Ray and Neutron Spectrometer (DraGNS) on the Dragonfly rotorcraft, which is currently in development and will start exploring Titan's surface in the mid-2030s [1, 2].

Our simulations indicate that neutrons from DraGNS pulsed neutron generator (PNG) and the multi-mission radiothermal generator (MMRTG) facilitate neutron spectroscopic measurements that characterize the surface to a depth of approximately ten cm. Because the PNG will be operated with a long neutron pulse length (nominally 90% duty cycle) as needed for DraGNS gamma-ray measurements, time domain neutron measurements (e.g. neutron die-away curves) will not be possible and we instead provide time-integrated measurements. These measurements meet all DraGNS neutron science requirements.

Neutron Physics: Neutron elastic scattering is the primary mechanism for thermalizing neutrons within Titan's surface. For surface irradiation with a pulsed neutron generator (14.1 MeV neutrons) or neutrons from a radioisotope thermal generator (~2 MeV neutrons), this process can lower the neutron energy by six to eight orders of magnitude. The macroscopic energy loss cross section, $\xi\Sigma_s$, provides a measure of neutron moderation within material comprised of multiple elements. Specifically, $\xi\Sigma_s$ is the sum of the abundance-weighted individual (microscopic)

moderation cross sections σ_s and is calculated as:

$$\xi\Sigma_s = N_A \sum_i \left(\xi_i \frac{w_i \sigma_{s,i}}{A_i} \right) \quad (1)$$

where N_A is Avogadro's number (6.022×10^{23} atoms mol⁻¹), ξ_i is the average logarithmic energy decrement per collision for element i , w_i is the weight fraction of element i , A_i is the atomic mass (in units of g mol⁻¹) of element i , and $\sigma_{s,i}$ is the individual (microscopic) neutron scattering cross section of element i in units of barns (1 b = 10^{-24} cm²). Higher $\xi\Sigma_s$ values mean more neutron moderation.

Following a sufficient number of elastic collisions, neutrons reach thermal equilibrium with the subsurface (mean energy of 0.012 eV) and scattering is no longer the dominant process for modifying the neutron population. Instead, neutron losses via absorption by nuclei are important, and the magnitude of the thermal neutron ($E_n < 0.5$ eV) flux is proportional to the total concentration of neutron absorbing elements as described by the macroscopic absorption cross section, Σ_a . Σ_a is the sum of the individual (microscopic), abundance-weighted absorption cross sections σ_a , and is calculated as:

$$\Sigma_a = N_A \sum_i \left(\frac{w_i \sigma_{a,i}}{A_i} \right) \quad (2)$$

where $\sigma_{a,i}$ is the individual (microscopic) neutron absorption cross section of element i in units of barns (1 b = 10^{-24} cm²).

Finally, following [3], we define the unitless quantity Δ as the ratio of the macroscopic absorption to macroscopic energy loss cross sections as:

$$\Delta = \frac{\Sigma_a}{\xi\Sigma_s} \quad (3)$$

$\xi\Sigma_s$, Σ_a , and Δ provide the basis for relating neutron measurements to surface compositions. This is shown in Figure 1A, which plots calculated $\xi\Sigma_s$ and Σ_a values for sixteen hypothetical Titan surface compositions derived from existing constraints, primarily from Cassini measurements (Figure 2).

Note that the compositions lie on a left-to-right trendline that corresponds to their relative concentration of the endmember materials water ice and ammonia. This dependency is strongly related to Σ_a , and is due to the significantly higher neutron-absorption cross section for N (1.90 b) as compared to H (0.33 b) and O (2×10^{-4} b). Vertical deviations from the water-ammonia mixing trendline are related to changes in neutron moderation resulting from variations in the H content of the material, and are a second-order effect.

Figure 1B plots the N/H wt. ratio of each composition versus Δ . N/H and Δ are highly correlated; no other element or ratio of elements provides a comparably robust correlation to Δ (or $\xi\Sigma_s$ and Σ_a).

Experimental Campaign: A prototype of the DraGNS neutron spectrometer is ready for a dedicated science measurement campaign. This instrument is composed of two ^3He -based neutron detectors (0.5” diameter, 17-cm-long active length, ^3He fill pressure of 20 atm). One sensor has a Cd wrap, making it sensitive to epithermal neutrons (energy > 0.3 eV), and by extension $\xi\Sigma_s$. The other (unwrapped) sensor is bare and the difference between it and Cd-covered sensors is inversely proportional to Σ_a . Simulations show that the correlation coefficients between measurements and neutron physics parameters is >0.95.

A variety of Titan surface analog materials are being prepared for this campaign, including water, polyethylene (CH_2), melamine ($\text{C}_3\text{H}_6\text{N}_6$), and melamine-doped epoxy bricks. The materials span the neutron physics parameters shown in Figure 1. The materials will be irradiated with neutrons, and neutron measurements will provide experimental validation of the physics-based relationships seen in Figure 1. In particular, we will confirm the measurement sensitivity to composition (e.g. correlation coefficients), measurement times (~5 mins for PNG neutrons, ~3 hrs for MMRTG neutrons) and measurement uncertainties.

References: [1] Lorenz, R.D., et al. 2018, *Johns Hopkins APL Technical Digest*, 34(3), p.14. [2] Barnes, J.W., et al. 2021, *Planet. Sci. Jour.* 2(4), p.130. [3] Feldman, W.C., et al. 2000, *J. Geophys. Res. Planets*, 105(E8), pp.20347-20363.

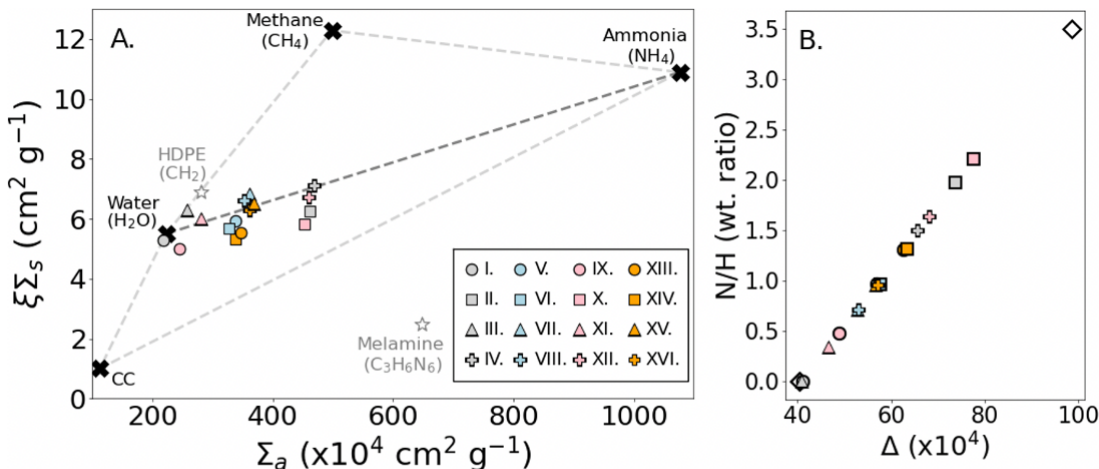


Figure 1. Behavior of the sixteen Titan surface composition case studies in the neutron parameter phase space. Black “x’s” indicate compositional endmembers, with dashed lines connecting them to aid the eye.

End-member compositions:	I. Primordial water ice flotation crust with admixed impactor material.	V. Frozen saline ammonia-water ocean water.	IX. Conglomerate of clasts of primordial water ice flotation crust and admixed impactor with matrix of tholin.	XIII. Conglomerate of clasts of frozen saline ammonia-water ocean with matrix of tholins.
	II. Primordial ammonia-water low-salinity eutectic melt with admixed impactor material.	VI. Frozen saline ammonia-water ocean water with admixed impactor.	X. Conglomerate of clasts of primordial ammonia-water low-salinity eutectic melt and admixed impactor with matrix of tholin.	XIV. Conglomerate of clasts of frozen saline ammonia-water ocean water and admixed impactor with matrix of tholins.
	III. Fragmental primordial water ice flotation crust with admixed impactor material, 30% pore space saturated with LCH ₄ .	VII. Fragmental frozen saline ammonia-water ocean water, 30% pore space saturated with LCH ₄ .	XI. Frags of conglomerate of clasts of primordial water ice flotation crust and admixed impactor with matrix of tholin, 30% porosity saturated with LCH ₄ .	XV. Frags of conglomerate of clasts of frozen saline ammonia-water ocean with matrix of tholins, 30% porosity saturated with LCH ₄ .
	IV. Fragmental primordial low-salinity ammonia-water eutectic melt with admixed impactor material, 30% pore space saturated with LCH ₄ .	VIII. Fragmental frozen saline ammonia-water ocean water with admixed impactor, 30% pore space saturated with LCH ₄ .	XII. Frags of conglomerate of clasts of primordial low-salinity ammonia-water eutectic melt and admixed impactor with matrix of tholin, 30% porosity saturated with LCH ₄ .	XVI. Frags of conglomerate of clasts of frozen saline ammonia water ocean and admixed impactor w/ matrix of tholin, 30% porosity saturated with LCH ₄ .

Figure 2. Overview of the hypothetical Titan compositions used for this study, and the key for interpreting the legend in Figure 1.